

Importance of the Sphingoid Base Length for the Membrane Properties of Ceramides

Terhi Maula,* Ibai Artetxe, Pia-Maria Grandell, and J. Peter Slotte

Biochemistry, Department of Biosciences, Åbo Akademi University, Turku, Finland

ABSTRACT The sphingoid bases of sphingolipids, including ceramides, can vary in length from 12 to >20 carbons. To study how such length variation affects the bilayer properties of ceramides, we synthesized ceramides consisting of a C12-, C14-, C16-, C18-, or C20-sphing-4-enin derivative coupled to palmitic acid. The ceramides were studied in mixtures with palmitoylphosphocholine (POPC) and/or palmitoylsphingomyelin (PSM), and in more complex bilayers also containing cholesterol. The *trans*-parinaric acid lifetimes showed that 12:1- and 14:1-PCer failed to increase the order of POPC bilayers, whereas 16:1-, 18:1-, and 20:1-PCer induced ordered- or gel-phase formation. Nevertheless, all of the analogs were able to thermally stabilize PSM, and a chain-length-dependent increase in the main phase transition temperature of equimolar PSM/Cer bilayers was revealed by differential scanning calorimetry. Similar thermal stabilization of PSM-rich domains by the ceramides was observed in POPC bilayers with a *trans*-parinaric acid-quenching assay. A cholestatrienol-quenching assay and sterol partitioning experiments showed that 18:1- and 20:1-PCer formed sterol-excluding gel phases with PSM, reducing the overall bilayer affinity of sterol. The effect of 16:1-PCer on sterol distribution was less dramatic, and no displacement of sterol from the PSM environment was observed with 12:1- and 14:1-PCer. The results are discussed in relation to other structural features that affect the bilayer properties of ceramides.

INTRODUCTION

Ceramides, which constitute one of the main intermediates in cellular sphingolipid metabolism, have been found to play important roles in cellular signaling processes (1–3), and the factors that form the basis of the biological effects of ceramides are receiving increasing attention. These sphingolipids are a minor but important component of biological membranes, and as a result of specific effectors, such as radiation, cytokines, and heat, the cellular amount of ceramides can increase remarkably (4). It is thought that changes in membrane structure and lateral organization induced by the specific interactions of ceramides with other cellular lipids or proteins participate in mediating the biological responses to increased levels of ceramides (5,6). In model membrane studies, it has been shown that ceramides can cause significant changes in the biophysical properties of phospholipid membranes by increasing their molecular order and inducing lateral phase separation (7–11). In more complex bilayers, ceramides can recruit sphingomyelin to form sphingolipid-enriched gel-phase domains (10,12,13), which at certain concentration ranges exclude cholesterol (CHL) (14,15). In the search for structural features that govern the biophysical properties and behavior of ceramides in bilayer membranes, most attention has been paid to the length and degree of unsaturation of the *N*-linked acyl chain (12,16–24) and the interfacial region close to the

polar head (19,25). Some studies have even included ceramides with different molecular species of the sphingoid bases, such as the phytosphingosine-based phytoceramide (19) and sphinganine-based dihydroceramide (26). To our knowledge, no studies have reported on the importance of the sphingoid base length in regulating the properties of ceramide bilayers, although great variation in the length of some sphingoid bases and sphingoid base-like compounds has been observed (27,28).

The enzymes responsible for the control of the length of cellular sphingoid bases, i.e., the serine palmitoyltransferases that catalyze the acylation of serine with palmitoyl-CoA in the *de novo* synthetic pathway of sphingolipids, are highly selective for fatty acyl-CoAs with 16 ± 1 carbon atoms, with the highest activity in the presence of palmitoyl-CoA (29–32). This accounts for the prevalence of sphingoid bases with 18 carbon atoms (16 from palmitoyl-CoA and two from serine). Although the C18-sphingoid bases sphingosine (sphing-4-enine), sphinganine, and phytosphingosine are by far the most common, in some animal tissues other chain-length variants predominate. For example, the gangliosides of mammalian brain (33) and human gastrointestinal mucosa (34), as well as equine kidney sphingolipids (35), contain substantial amounts of C20-sphingoid bases. Shorter sphingoid bases can be found in relatively high amounts in, e.g., bovine sphingolipids (36–38) and the skin of the Antarctic minke whale (39), which contain sphingoid bases with 16 carbon atoms. Moreover, insect sphingolipids contain primarily shorter sphingoid bases (C14 and C16) (40,41). A strikingly wide range of different sphingoid base lengths is found in the ceramides of human skin, ranging from as short as C12- (42) to as long as C28-sphingoid bases (43).

Submitted June 5, 2012, and accepted for publication September 11, 2012.

*Correspondence: terhi.maula@abo.fi

Ibai Artetxe's present address is Unidad de Biofísica (Centro Mixto CSIC-UPV/EHU), and Departamento de Bioquímica, Universidad del País Vasco, Bilbao, Spain.

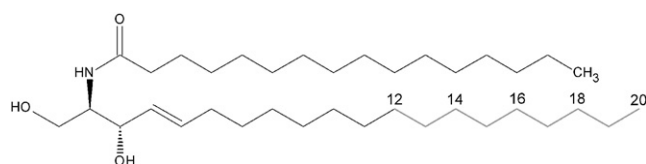
Editor: Klaus Gawrisch.

Fyrst and co-workers (41), who characterized the sphingoid bases of *Drosophila melanogaster*, suggested that short-chain sphingoid bases are likely to have significantly different biophysical properties compared with longer-chain sphingoid bases. Moreover, they suggested differences in the effects that sphingoid bases of varying length could have on membranes. To further develop this hypothesis, we synthesized ceramides in which the length of sphingosine was systematically shortened from 20 to 12 carbons (Scheme 1), and investigated the membrane properties of these ceramides in two-component liposomes with palmitoyloleoylphosphocholine (POPC) or (hexadecanoyl)-sphing-4-enine-1-phosphocholine (palmitoylsphingomyelin, PSM), and in more complex bilayers composed of POPC, PSM, and ceramide, both with and without CHL. The length of the sphingoid base was observed to markedly affect the membrane behavior of the ceramides in terms of interlipid interactions and formation of ceramide-rich ordered- or gel-phases. The results are discussed in relation to other structural features that have been found to be important for the bilayer properties of ceramides.

MATERIALS AND METHODS

PSM was purified from egg yolk sphingomyelin (Avanti Polar Lipids, Alabaster, AL) as previously described (44). (hexadecanoyl)-sphing-4-enine (palmitoylceramide, 18:1-PCer) was purchased from Larodan Fine Chemicals (Malmö, Sweden). (hexadecanoyl)-dodecaspheing-4-enine (12:1-PCer), (hexadecanoyl)-tetradecaspheing-4-enine (14:1-PCer), (hexadecanoyl)-hexadecaspheing-4-enine (16:1-PCer), and (hexadecanoyl)-icosaspheing-4-enine (20:1-PCer) were synthesized by coupling the different length *D-erythro*-sphingoid bases (dodecaspheing-4-enine, tetradecaspheing-4-enine, hexadecaspheing-4-enine, or icosaspheing-4-enine; Larodan Fine Chemicals) to palmitic anhydride (Sigma-Aldrich, St. Louis, MO) as described previously (45) (Scheme 1). All other synthetic procedures and sources of the commercial chemicals are described in the Supporting Material.

To obtain information about the properties of binary bilayers of POPC and the ceramide analogs (at 85/15 mol %), or quaternary bilayers of POPC/PSM/Cer/CHL (60/15/15/10 mol %), we measured the fluorescence lifetimes of *trans*-parinaric acid (tPA, at 0.5 mol %) in multilamellar vesicles at 23°C. Differential scanning calorimetry (DSC) was used to study the thermotropic properties of PSM/Cer bilayers of equimolar composition. The effects of the ceramide analogs on the thermal stability of PSM-rich ordered domains were studied in ternary bilayers of POPC/PSM/Cer (70/15/15 mol %) with a tPA-fluorescence quenching assay (22). Possible displacement of sterol from the PSM-rich environment in POPC/PSM/



SCHEME 1 Schematic representation of the ceramide analogs used in this study. The ceramides differed in the length of the sphingoid base (12, 14, 16, 18, or 20 carbon atoms) that was based on the sphing-4-enine (sphingosine) structure. All ceramides contained palmitic acid as the *N*-linked acyl chain.

Cer/CHL bilayers (60/15/15/10 mol %) was studied with a cholestatrienol (CTL)-fluorescence quenching assay (46). Fluorescence quenching was measured in phase-separated multilamellar vesicles as a function of temperature, and determined as the relative fluorescence intensity of the fluorescent probes (1 mol % of tPA added to the bilayers or 1 mol % of CTL replacing an equal amount of CHL) in quenched F samples, which contained both the probe and the quencher (i.e., 1-palmitoyl-2-stearoyl-(7-doxyl)-*sn*-glycero-3-phosphocholine (7SLPC) that replaced an equal amount of POPC), over the intensity from unquenched F₀ samples, which contained the fluorophores but no quencher. Increasing the temperature in the samples changed the quenching susceptibility of the probes by increasing the solubility of 7SLPC in the laterally segregated domains enriched in the probes as the bilayers became more disordered. Domain melting was observed as a gradual decrease in the F/F₀ ratio. To determine the affinity of sterol for bilayers containing the ceramide analogs, we measured the partitioning of CTL (2 mol %) between methyl- β -cyclodextrin ($m\beta$ CD) and unilamellar vesicles composed of POPC/PSM/Cer/CHL (60/15/15/10 mol %). The molar fraction partition coefficient (K_x) of CTL was obtained as previously described (20,47). All methods are described in more detail in the Supporting Material.

RESULTS

Effects of the ceramide analogs on fluid POPC bilayers

Long-chain ceramides are known to induce lateral phase separation in fluid phosphatidylcholine bilayers, with the concomitant formation of ceramide-rich ordered- or gel-phase domains (7–11). To study the ability of the long-chain base modified ceramides to form ordered phases in fluid POPC bilayers at 23°C, we measured the fluorescence decays of tPA in POPC containing 15 mol % of ceramide (Fig. 1). In general, tPA displays short lifetimes in phases of low packing densities, whereas its lifetime components become significantly longer in phases of high molecular order, with a fingerprinting lifetime of ≥ 30 ns reported

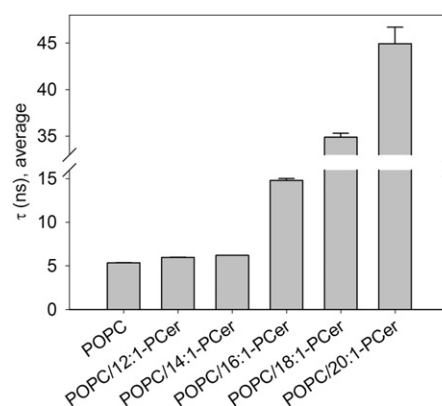


FIGURE 1 Effect of the ceramide analogs on the order of POPC bilayers. The mean fluorescence lifetimes of tPA (0.5 mol %) were measured in multilamellar vesicles composed of POPC or POPC/Cer (85/15 mol %, 100 μ M final lipid concentration) at 23°C. The mean lifetime of tPA in the presence of 12:1- and 14:1-PCer was close to that of pure POPC, whereas 16:1-, 18:1-, and 20:1-PCer induced a chain-length-dependent increase in the mean lifetime. The average intensity-weighted lifetimes \pm SD for triplicates are shown.

for ceramide-containing gel-phases (11,48–50). The 5 ns mean lifetime of tPA in POPC bilayers was only weakly affected by the presence of 12:1- and 14:1-PCer, both of which increased the lifetime to ~6 ns (Fig. 1). Such short lifetimes signify efficient spontaneous quenching of tPA due to the bilayers being in a disordered state. The presence of 16:1-, 18:1-, and 20:1-PCer increased the mean lifetime of tPA to 15 ns, 35 ns, and 45 ns, respectively, indicating a significant increase in the order of the POPC bilayers (Fig. 1).

An inspection of the individual lifetime components of tPA revealed that whereas in pure POPC and mixtures of POPC and 12:1- or 14:1-PCer, two short lifetimes occurred, the presence of 16:1-, 18:1-, and 20:1-PCer gave rise to a third, long component above 30 ns (see the data for binary mixtures in Table S1). The length, intensity, and amplitude of this long component increased with increasing sphingoid base length. For the POPC/18:1-PCer bilayers at the applied molar fraction of ceramide (15 mol %), the long-lifetime component is related to the existence of a ceramide-rich gel-phase (11,48). Thus, the results suggested lateral segregation and formation of ceramide-rich ordered- or gel-phases also by 16:1- and 20:1-PCer. The appearance of the long-lifetime component was accompanied by a slight increase in the length of the shorter components (Table S1), reflecting an ability of the long-chain ceramides to enhance the acyl chain packing of POPC, as previously shown for 18:1-PCer (9,11).

Thermotropic properties of PSM/ceramide analog bilayers

To obtain information about the effects of the sphingosine length on ceramide interactions with PSM, we performed DSC studies with multilamellar vesicles composed of binary (1:1) mixtures of the ceramide analogs and PSM (Fig. 2). The ceramide analogs were found to interact with PSM to form gel-phases with higher gel-to-fluid transition temperatures than observed with pure PSM (41°C). A chain-length-dependent increase in the thermal stability of the gel-phases was observed, with main phase transition temperatures of 46°C, 52°C, 65°C, 72°C, and 71°C for increasing sphingosine length on ceramide (Fig. 2, lines 2–6). The 12:1 and 14:1 analogs also reduced the enthalpy of the PSM pretransition (at ~30°C), whereas it was fully diminished by the other ceramide analogs. Separate melting transitions for PSM and the ceramides were not observed in any of the mixtures. The main phase transition temperature observed for the PSM/18:1-PCer bilayers (72°C) agrees well with previously reported values for the same binary composition (25,46,51). When Busto and co-workers (51) analyzed this particulate mixture, the peak at 72°C was deconvoluted into two components with presumable differences in the relative PSM/ceramide ratios. Thus, the DSC profiles shown in Fig. 2 probably represent melting of complex gel phases

with differences in the relative proportions of PSM and ceramide. Because the detailed composition of each gel-phase component is unknown, it is difficult to discuss the partitioning of the ceramides in the mixed phases in detail. In conclusion, although the 12:1- and 14:1-PCers failed to increase the order of fluid POPC bilayers (Fig. 1), they were still able to interact with PSM to form high-melting-temperature gel-phases (Fig. 2). The difference in the ability of these ceramides to increase the relative order of POPC and PSM could originate partly from the higher proportion of the ceramides in the PSM bilayers, but it could also relate to ceramide favorably partitioning into sphingomyelin-rich domains in bilayer membranes (8,13,46,52), reflecting more favorable interactions between ceramide and sphingomyelin.

Effect of the ceramide analogs and CHL on the thermal stability of PSM-rich gel-phase domains in POPC bilayers

To study whether the ceramide analogs also interacted with PSM in ternary mixtures with POPC, where lateral phase separation is expected, and to compare the effects of the ceramides and CHL on the thermostability of PSM-rich gel-phase domains in POPC bilayers, we performed tPA-fluorescence quenching studies in ternary mixtures of POPC/PSM/Cer or CHL (70/15/15 mol %; Fig. 3). Because tPA preferentially partitions into ordered phases (11,49), it

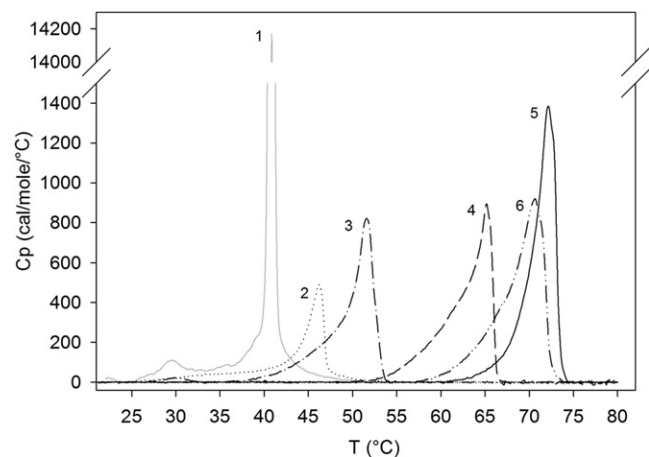


FIGURE 2 Thermotropic properties of PSM/ceramide binary bilayers. DSC thermograms of pure PSM and equimolar PSM/Cer binary mixtures (1 mM final lipid concentration) were recorded between 20°C and 95°C at a temperature gradient of 1°C/min. The ceramide analogs interacted with PSM to form complex gel phases for which the transition temperature increased in a chain-length-dependent manner. Representative data of the highest phase transition peaks of the second heating scans of four independently repeated experiments are shown for 1), PSM; 2), PSM/12:1-PCer; 3), PSM/14:1-PCer; 4), PSM/16:1-PCer; 5), PSM/18:1-PCer; and 6), PSM/20:1-PCer. For clarity, only the temperature range around the main gel-to-fluid transition for each mixture is shown, and stretches that showed no remarkable features are omitted.

is suitable for detecting changes in the thermal stability of sphingolipid-rich domains in heterogeneous bilayers (22,25). The ceramide analogs were observed to induce a chain-length-dependent thermal stabilization of PSM-rich domains in the POPC bilayers (Fig. 3). In the absence of ceramide (or CHL) the PSM-rich domains melted at $\sim 16^\circ\text{C}$ (Fig. 3, bottom trace). This observation agrees well with the reported phase diagrams for this mixture, which show that up to 14°C a fluid and a PSM-rich gel-phase coexist in the bilayers, whereas at higher temperatures the bilayers are in a fully fluid state (48,53,54). When 15 mol % of the ceramide analogs was added to the bilayers, the domain-melting temperature increased in proportion to the sphingoid base length, occurring at $\sim 20^\circ\text{C}$, 28°C , 40°C , 47°C , and 50°C (Fig. 3). This finding agrees well with the thermal stabilization of the PSM gel phase observed with DSC (Fig. 2). In the ternary bilayers containing 18:1-PCer, the high end-melting temperature observed in Fig. 3 stems from the melting of a ceramide-rich gel phase that coexists with a POPC-rich fluid phase (48).

When 15 mol % of CHL was added to the bilayers, tPA reported a domain melting at $\sim 29^\circ\text{C}$, indicating that CHL was more pronounced than 12:1-PCer and nearly equal to 14:1-PCer in its ability to thermally stabilize the PSM-rich domains. However, the affinity of tPA for the domains seemed to be higher in the presence of the ceramides than with CHL, as evidenced by the larger shift in the F/F_0 amplitude. This is most probably attributed to the higher total proportion of sphingolipids compared with the CHL-containing bilayers. The thermal stabilization induced by the ceramide analogs with longer than C14 sphingosines was significantly greater than that induced by CHL, reflecting stronger interactions of those ceramides with PSM.

Formation of sterol-excluding ordered or gel-phases by PSM and the ceramide analogs in complex bilayers

After observing that in POPC bilayers the ceramide analogs were all able to interact with PSM to form sphingolipid-rich domains (Fig. 3), we decided to study how the formation of such domains affected the lateral distribution of CHL in complex mixtures. To that end, we performed CTL-fluorescence quenching studies in ternary and quaternary mixtures of POPC/PSM/CHL and POPC/PSM/Cer/CHL (Fig. 4). We previously reported the successful use of the CTL-quenching assay to study the formation and thermal stability of CHL-rich domains in heterogeneous bilayers (46). Ceramides have been shown to induce displacement of CHL from sphingomyelin-rich or saturated phosphatidylcholine-rich domains (14,15,46,55,56), and in such situations no sterol-rich domains are reported by the CTL-quenching assay (14,46). We studied the effects of the ceramide analogs on formation of sterol-rich domains by comparing the CTL-quenching in POPC/PSM/CHL bilayers

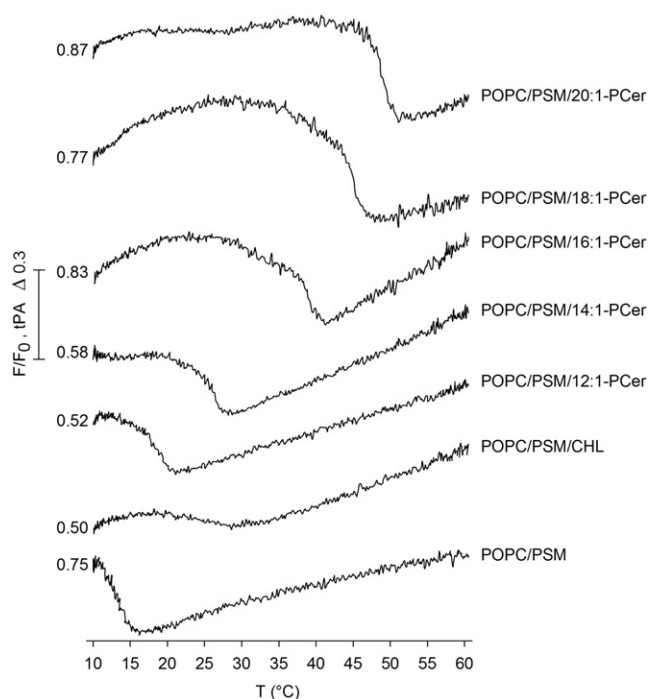


FIGURE 3 Effect of the ceramide analogs on the melting of PSM-rich domains in POPC bilayers. 7SLPC-induced fluorescence quenching of tPA as a function of temperature was measured in multilamellar vesicles with $50\ \mu\text{M}$ final lipid concentration. The vesicles were composed of POPC/PSM (82/18 mol %), POPC/PSM/CHL (70/15/15 mol %), and POPC/PSM/Cer (70/15/15 mol %). F/F_0 was defined as the relative fluorescence intensity of tPA in the F samples that contained both 7SLPC (replacing 50% of POPC) and tPA (1 mol %) over the intensity in the F_0 samples that contained tPA (1 mol %) but no 7SLPC. tPA-quenching revealed that each of the ceramide analogs was able to thermally stabilize the PSM-rich domains in fluid POPC bilayers. However, compared with CHL, only 16:1-, 18:1-, and 20:1-PCer were more pronounced in their ability to increase the end-melting temperature of the PSM-rich domains. As a reference to the relative changes in the F/F_0 between the different mixtures, the initial F/F_0 value is given for each measurement. Representative curves of two independently repeated experiments are shown.

of 60/30/10 molar composition with that observed when half of the PSM was replaced with a ceramide (to yield POPC/PSM/Cer/CHL, 60/15/15/10 mol %). The melting profile of the POPC/PSM/CHL 75/15/10 molar composition is shown as a reference for bilayers with a reduced amount of PSM but no ceramide. The melting of the gel phase that is known to be present in the POPC/PSM/CHL mixture at 60/30/10-molar composition at 23°C (53,54) is clearly shown in the CTL-quenching profile, with an apparent end-melting temperature of $\sim 38\text{--}40^\circ\text{C}$ (Fig. 4, uppermost trace). However, when half of the PSM in those bilayers was substituted by 18:1- or 20:1-PCer, CTL was quenched already at low temperatures and no domain melting could be observed. This suggested the formation of highly ordered PSM/ceramide-rich domains that excluded sterol, which has been shown to be the case for 18:1-PCer in bilayers equal to those studied here (14,25,46). Although the initial F/F_0

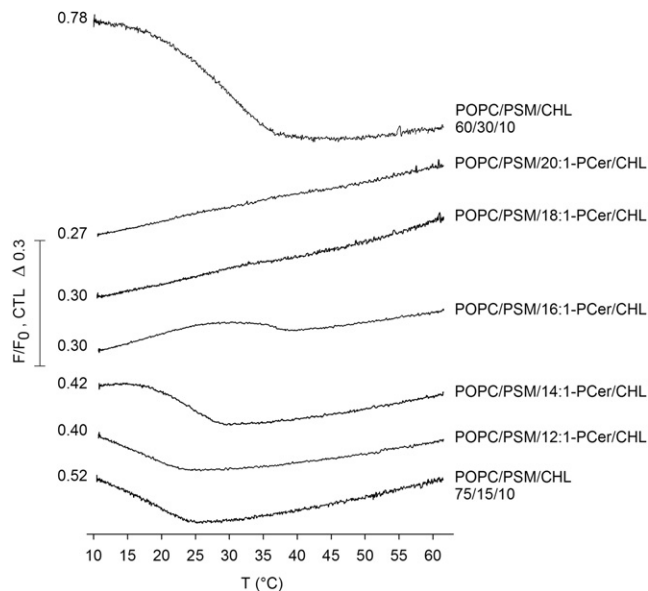


FIGURE 4 Effect of the ceramide analogs on sterol-enriched domains in complex bilayers. 7SLPC-induced fluorescence quenching of CTL as a function of temperature was measured in multilamellar vesicles with 50 μM final lipid concentration. The vesicles were composed of POPC/PSM/CHL (60/30/10 or 75/15/10 mol %) or POPC/PSM/Cer/CHL (60/15/15/10 mol %). F/F_0 was defined as the relative fluorescence intensity of CTL in the F samples that contained both 7SLPC (replacing 50% of POPC) and CTL (replacing 1 mol % of CHL) over the intensity in the F_0 samples that contained CTL (replacing 1 mol % of CHL) but no 7SLPC. CTL-quenching revealed that when PSM and 18:1- or 20:1-PCer existed in the bilayers at an equimolar amount, sterol was displaced from the PSM environment and no domain melting was observed. Displacement of sterol was verified by the existence of PSM/ceramide-rich, high-melting-temperature, gel-phase domains in those bilayers (Fig. S1 and Table S1). The POPC/PSM/CHL 75/15/10 molar composition is shown as a reference for bilayers with a reduced amount of PSM but no ceramide. As a reference to the relative changes in the F/F_0 between the different mixtures, the initial F/F_0 value is given for each measurement. Representative curves of at least three independently repeated experiments are shown.

ratio of CTL emission in the presence of 16:1-PCer was as low as that in the presence of 18:1- and 20:1-PCer (Fig. 4), signifying efficient initial quenching of CTL fluorescence, the observation of a domain melting at $\sim 38^\circ\text{C}$ indicated that a fraction of CTL was still protected against quenching, and that 16:1-PCer did not completely displace sterol from the PSM environment in those bilayers.

In the presence of 12:1- and 14:1-PCer, the CTL quenching reported domain meltings at $\sim 23^\circ\text{C}$ and 29°C , respectively (Fig. 4). Such clear melting profiles indicated that these ceramides were not able to interact with PSM in the quaternary bilayers so as to form sterol-excluding sphingolipid-rich domains. Moreover, the similarity of the melting profiles in the presence of 12:1- and 14:1-PCer to that of the POPC/PSM/CHL 75/15/10 bilayers (Fig. 4, bottom trace), in which half of the original 30 mol % of PSM was replaced with POPC, suggested that instead of interacting with PSM, the ceramides could even have

partitioned more into the POPC-rich phase, increasing the proportion of the fluid phase in the bilayers. Alternatively, they could have coexisted with PSM in the sterol-rich domains, in which case the 12:1-PCer did not greatly affect their thermal stability, whereas a slight thermal stabilization was induced by 14:1-PCer.

We previously suggested that the displacement of CHL from PSM-rich domains is dependent on the ability of ceramide to thermally stabilize and increase the order of the PSM environment (14,25). Although all of the ceramide analogs were observed to thermally stabilize PSM in the binary and ternary mixtures (Figs. 2 and 3), differences in their ability to interact with and affect the molecular order of PSM-rich domains in the complex bilayers could explain the observed differences in their ability to form sterol-excluding sphingolipid-rich domains. Indeed, when we used tPA-quenching to detect the effects of the ceramides on the melting of PSM-rich domains in bilayer compositions equal to those used in the CTL-quenching experiment, only 18:1- and 20:1-PCer were observed to thermally stabilize the PSM environment (Fig. S1). This finding is consistent with that of Chiantia and co-workers (12), who studied the effect of the *N*-acyl chain length on the formation of ceramide-rich phases and observed that only long-chain ceramides were able to segregate into ceramide-rich domains in complex bilayers. The 18:1 and 20:1 analogs also significantly increased the mean lifetime of tPA in the complex bilayers (Fig. S2), an effect attributed to the increase in both length and amplitude of the longest-lifetime component of tPA, indicating increased proportion of gel-phase in the presence of these ceramides compared with the bilayers with 30 mol % of PSM (Table S1). For the complex bilayers containing 12:1-, 14:1-, and 16:1-PCer, tPA-quenching reported domain-melting temperatures similar to those observed with CTL (Fig. 3 and Fig. S1), indicating that the two probes detected the same domains in those bilayers. Clearly, 12:1- and 14:1-PCer were not able to recruit PSM to formation of sphingolipid-rich domains of high thermal stability or high molecular order (Fig. S1 and Fig. S2), which explains why these ceramides were not observed to displace sterol from the PSM environment. Whether 12:1- and 14:1-PCer partitioned more into the POPC-rich fluid phase or were associated with the PSM/sterol-rich domains in the complex bilayers remains unresolved. However, a comparison of the individual lifetime components of tPA in the complex mixtures revealed that the lifetimes of tPA were longer in the 14:1-PCer-containing bilayers than in the POPC/PSM/CHL bilayers with 15 mol % of PSM, indicating that the presence of 14:1-PCer increased the molecular order of the PSM-rich domains (Table S1). With the methodology used in this study, we cannot distinguish whether this effect stemmed from 14:1-PCer being located in the PSM-rich environment (without displacing sterol) or if this ceramide had a more indirect effect on the domains from the fluid phase (e.g., at the

domain boundaries). Although 16:1-PCer was not observed to thermally stabilize the PSM-rich domains or to increase the mean lifetime of tPA in complex mixtures such as 18:1- and 20:1-PCer (Fig. S1 and Fig. S2), it induced an increase in the longest-lifetime component of tPA when it substituted half of the PSM in the 60/30/10-mixture (Table S1), indicating an increase in the molecular order of the PSM-rich phase. However, the length, intensity, and amplitude of the longest-lifetime component with 16:1-PCer were significantly lower than with 18:1- and 20:1-PCer, suggesting that the gel-phase-forming properties of 16:1-PCer were remarkably attenuated compared with those of the ceramides with longer sphingoid bases. This explains why 16:1-PCer was not as effective as 18:1- and 20:1-PCer in displacing CHL. The low initial F/F_0 observed with 16:1-PCer in the CTL-quenching assay (Fig. 4), as well as the low F/F_0 amplitude observed with tPA quenching (Fig. S1), suggests low affinity of the probes for the domains formed in the presence of 16:1-PCer. However, because the quenching assay is based on collisional quenching of the fluorophores in phase-separated bilayers where POPC is expected to have a fluidizing effect on domain boundaries, domains of smaller size or increased proportion of domain boundary would be less efficient in protecting the fluorophores from quenching than larger domains or domains in which the boundary line is minimized, resulting in low F/F_0 initial values and amplitude shifts. Thus, the domains in the presence of 16:1-PCer could be smaller in size or of a different shape than those formed by, e.g., the 18:1 and 20:1 analogs, which could have affected the amplitude of the quenching.

Effects of the ceramide analogs on bilayer affinity of sterol

To gain additional insight into the effects of the ceramide analogs on the bilayer distribution of sterol, we measured the bilayer affinity of CTL in the complex bilayers at 23°C and 37°C (Fig. 5). The CTL-partitioning assay provides information about the overall bilayer affinity of sterol in equilibrium conditions and has been successfully used to report on changes in sterol affinity in the presence of ceramides (20,22,25). In contrast to the CTL-quenching assay, which provides information about the formation and thermal stability of laterally segregated sterol-rich domains, the partitioning assay measures the molar partition coefficient (K_x) of sterol for the whole bilayer, and thus can reveal ceramide-induced changes independently of the lateral distribution of the ceramides in the bilayers. Sterol was observed to partition more favorably into bilayers that contained PSM than into pure POPC bilayers at both measured temperatures (Fig. 5), which is consistent with similar data for comparable systems (20,57). For the PSM-containing bilayers (at both 60/30/10 and 75/15/10 molar composition), sterol affinity was lower at 37°C than at 23°C, reflecting less favorable partitioning of sterol to the bilayers when they were in a more fluid state.

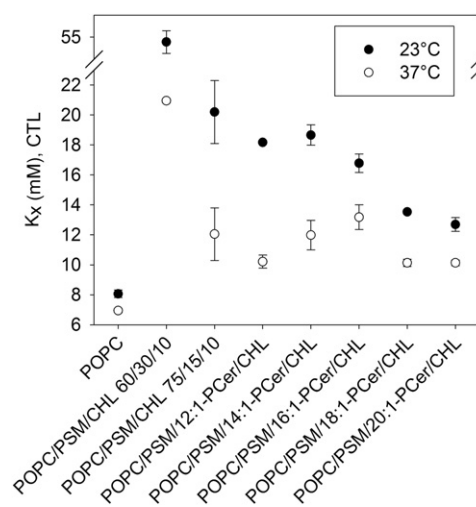


FIGURE 5 Bilayer affinity of sterol in the presence of the ceramide analogs in complex bilayers. The affinity of CTL (2 mol %) for unilamellar vesicles composed of POPC, POPC/PSM/CHL (60/30/10 or 75/15/10 mol %), and POPC/PSM/Cer/CHL (60/15/15/10 mol %) was deduced from the equilibrium partitioning of CTL between the vesicles (40 μ M final lipid concentration) and m β CD at 23°C (solid circles) and 37°C (open circles). Sterol affinity was defined as the molar fraction partition coefficient $K_x \pm$ SD for duplicate measurements as previously described (47).

We previously showed that sterol displacement from a PSM-rich environment has a remarkable reducing effect on the bilayer affinity of sterol (25). Therefore, replacement of half of the PSM in the POPC/PSM/CHL bilayers (60/30/10 molar composition) by 18:1- or 20:1-PCer, which were shown to displace sterol from the PSM-rich domains (Fig. 4), is expected to cause a marked reduction in sterol affinity, which was shown to be the case (Fig. 5).

Consistent with the partial sterol displacement induced by 16:1-PCer (Fig. 4), the reduction in sterol affinity was not as steep in the presence of 16:1-PCer as with the longer ceramides. For the bilayers that contained 12:1- or 14:1-PCer, the low sterol affinity was not caused by sterol displacement, but rather was a result of a reduction in the amount of PSM. This conclusion is supported by the observation that the level of sterol affinity in the presence of those ceramides was similar to that observed for the POPC/PSM/CHL 75/15/10 bilayers (Fig. 5). 12:1- and 14:1-PCer could have partitioned into the POPC-rich phase, or coexisted with CHL in the PSM-rich domains, without significantly affecting the affinity of CTL for the PSM-rich domains in the bilayers. Another interesting finding was the gradual increase in sterol affinity at 37°C when the sphingoid base of ceramide increased from 12 to 16 carbons. This effect could be related to the gradually increasing stabilizing effect of the ceramides on the PSM-rich domains observed in Fig. 3.

DISCUSSION

Different targeted modifications of ceramide molecules have been widely used to reveal how the structure of these

molecules affects their membrane behavior, and which features of the structure govern their bilayer properties. However, to our knowledge, no studies about the importance of the long-chain base length in regulating the properties of ceramides in bilayers have been reported, although animal sphingolipids have been found to contain sphingoid bases with a wide range of varying lengths (27,28). In this study we examined the membrane effects of ceramide analogs with C12-C20 sphingosine bases (Scheme 1). In general, our results show that in addition to the features reported earlier regarding the *N*-acyl chain (12,16–23) and the interface region (19,25), the membrane behavior of ceramides is also markedly affected by the length of their sphingoid base when the *N*-linked acyl chain length is kept unchanged.

For saturated phospholipids, reducing the number of carbon atoms on either of the hydrocarbon chains causes a decrease in the chain melting temperature (58). Because the sphingoid base and the *N*-acyl chain of ceramides can be considered to be similar to the hydrocarbon chains of phospholipids, it is not surprising that effective shortening of the length of the sphingosine, and the subsequent induction of chain mismatch, was found to affect the bilayer properties of the ceramide analogs in terms of interactions with other membrane lipids. Nevertheless, the differences observed in the membrane behavior of the ceramide analogs provide interesting insights into the importance of the sphingoid base length for the membrane effects of ceramides. This study by no means provides a thorough characterization of the interlipid interactions, bilayer behavior, or phase state of the ceramide analogs; rather, it is a preliminary study about the relative effects of the sphingoid base length on the membrane properties of ceramides. For the mixtures containing ceramide analogs other than palmitoylceramide (18:1-PCer), the phase behavior or relative amount of gel-like or ordered domains is not known, but the observation of formation and relative order of such domains, together with the observed effects on other bilayer properties (such as molecular order and sterol distribution), still enable a comparison of the overall properties of the different mixtures.

Effect of the sphingoid base length on ceramide properties in two-component bilayers

Considering the perpendicular orientation of the axes of the ceramide hydrocarbon chains toward the planar, rigid amide link (59), one would expect the two aliphatic chains to protrude in a similar way into the membrane, having similar properties in the membrane hydrophobic core. Long, saturated ceramide acyl chains confer a high degree of order to the center of the membrane, and therefore varying the length of either of the chains, causing mismatch-induced disordering effects on the terminal carbons and reduced chain-chain van der Waal's interactions would be expected to have similar effects on the bilayer properties of ceram-

ides. This seems to be true for the interactions of ceramides with sphingomyelin in binary bilayers. Here, our DSC studies with PSM/Cer (1:1) mixtures revealed that shortening of the sphingosine length of ceramide induced a chain-length-dependent decrease in the gel-to-fluid transition temperature of the complex gel phases that all of the analogs formed with PSM (Fig. 2). In a previous study (16), we observed a similar chain-length-dependent effect on the thermotropic properties of PSM when ceramides with different *N*-acyl chain lengths were mixed with PSM in two-component liposomes (though with lower concentrations of ceramides than were used here).

The high degree of asymmetry in the melting transitions of the PSM/ceramide mixtures shown in Fig. 2 raises a question as to whether they could represent overlapping transitions instead of melting of a complex PSM/ceramide-gel phase. Due to limitations in the availability of the analogs, we did not record the thermograms of the pure ceramide components. However, because ceramides that contain short or intermediate-length *N*-acyl chains display relatively high melting temperatures (e.g., 54°C for C2 (18) and 64.4°C for C8 ceramide (16)), we believe that the melting transitions of the pure ceramide analogs would occur at much higher temperatures than the melting of the corresponding mixtures with PSM shown in Fig. 2. Thus, we consider it safe to assume that the DSC-melting profiles represent the melting of the mixed PSM/ceramide-gel phases.

Although our ceramide analogs were all able to interact with PSM in the binary bilayers (Fig. 2), chain-length-dependent differences were observed in the miscibility of the ceramides in fluid POPC bilayers (Fig. 1 and Table S1). Only the analogs with C16 or longer sphingosine were observed to induce ordered- or gel-phase formation in POPC bilayers. In a previous study, Karttunen and co-workers (61) observed a chain-length-dependent lateral phase separation for ceramides with varying *N*-acyl chain lengths in fluid dimyristoyl-PC monolayers. They found that ceramides with *N*-acyl chains as short as C10 phase-separated from the PC. If 18:1-PCer is considered structurally symmetric (in accordance with the calculations of Kodama and Kawasaki (62) demonstrating the symmetry of palmitoylsphingomyelin), then a 10-carbon-long *N*-acyl chain would correspond to a 12-carbon-long sphingosine. However, neither 12:1-PCer nor 14:1-PCer was found to phase-separate from POPC in our study (Fig. 1 and Table S1).

Effect of the ceramide analogs upon CHL distribution and formation of ordered domains in complex lipid systems

We previously showed, using tPA- and CTL-quenching assays similar to those used here, that a minimum length of 8 carbons for the *N*-acyl chain was required for ceramide to displace CHL from a PSM-rich environment (17).

However, in the study presented here, we show that the minimum length requirement of the sphingosine for ceramide to displace sterol was 16 carbons (corresponding roughly to 14 carbons in the *N*-acyl chain), and even then the displacement was not nearly as effective as that obtained by ceramides with longer sphingosines (Fig. 4). These observations indicate that the sterol-displacing capability of ceramides is more sensitive to shortening of the sphingoid base than to shortening of the *N*-acyl chain. Clearly, the ability of the sphingoid-base-modified ceramides to displace sterol from the PSM-rich phase was related to their ability to recruit PSM into ceramide-rich ordered- or gel-phase domains (Fig. 4 and Fig. S1). Similarly, a possible ceramide-induced displacement of CHL from a sphingomyelin-rich phase was previously proposed for ceramides with an *N*-acyl chain long enough to enable formation of ceramide-rich phases (12). We also showed in an earlier study (20) that the efficacy of ceramide in interfering with the lateral distribution and overall bilayer affinity of sterol is dependent on the *N*-acyl chain length. In that study, ceramides with relatively long *N*-acyl chains (C16 and C18) were shown to effectively reduce the bilayer affinity of sterol. Similarly, here we observed the most efficient reduction in sterol affinity with ceramides that contained the longest sphingosines (C18 and C20; Fig. 5). The methodology used in this study does not allow us to safely conclude what the lateral localization of 12:1- and 14:1-PCer was in the complex mixtures, but it was evident that they were not able to increase the thermal stability and molecular order of the PSM-rich phase enough to interfere with the lateral distribution of CHL (Fig. 4 and Fig. S1). However, it was previously shown that ceramides with short *N*-acyl chains mix with lipids in a sphingomyelin/CHL-rich phase in complex lipid mixtures similar to those used in this study (12).

Possible effects of chain mismatch on ceramide molecular shape and lateral chain packing

When Megha and co-workers (19) compared two groups of ceramide derivatives, one with different small structural modifications of the sphingoid base near the headgroup region and one with varying *N*-acyl chain lengths, they observed that the structural modifications did not affect the bilayer properties of the ceramides nearly as much as did shortening the *N*-acyl chain length. Therefore, they suggested that ceramide packing in bilayers is more sensitive in the hydrophobic core of the membrane than in the polar headgroup region. Our results also emphasize the importance of two long chains for more thermostable chain packing of ceramides. However, it is known that the extensive network of interfacial hydrogen bonds that ceramides form in bilayers has a major impact on their bilayer properties (59), and that impairing hydrogen bonding and interfacial packing at the amide-link nitrogen limits the lateral

packing interactions of ceramides (25). Therefore, shortening of the sphingosine may also have caused altered geometry and subsequent conformational changes that affected both the van der Waals interactions between the ceramide acyl chains and the packing properties of the ceramides at the interfacial level.

The more-fluid nature observed for the ceramides when the degree of chain mismatch was increased could also depend on an increase in the surface area occupied by the ceramides. With regard to sphingomyelins experiencing chain mismatch caused by the *N*-acyl chain extending beyond the length of the sphingoid base, it has been suggested that rotational motions of the shorter sphingoid base exert a disordering effect on the mismatched bonds in the adjacent *N*-acyl chain, increasing the likelihood of gauche rotamers in the terminal part of the *N*-acyl chain (62). This, again, has been suggested to explain why the sphingomyelin gel phase becomes destabilized in mismatched sphingomyelin bilayers (63). Likewise, the mismatch induced by shortening of the sphingoid base could perturb the conformation of the ceramide acyl chains, affecting their interlipid interactions. It has been suggested for ceramides with varying *N*-acyl chain lengths that chain mismatch prevents the acyl chains of asymmetric ceramides from adopting a conformation that maximizes the chain-chain interactions, with the bulky terminal methyl of the mismatched chains occupying a wider volume than the chains of symmetric ceramides (64). Hydrophobic mismatch of the acyl chains has been shown to cause partial interdigitation and complex miscibility behavior of ceramides, features that can affect the lateral partitioning of lipids (64,65). Moreover, saturation of the C4-C5 double bond in sphingosine, which locates near the functional groups (i.e., the amide-link nitrogen and the C3-hydroxy group) has been shown to affect the lateral packing behavior of ceramide, leading to less dense packing of the ceramide acyl chains (26,66). In light of this, shortening of the sphingosine may also have induced orientational disorder about the C4-C5 double bond, increasing the lateral space requirement of ceramide and causing perturbations in the interactions of the ceramide analogs with neighboring lipid acyl chains. In monolayers, the mean molecular areas of ceramides with an *N*-acyl chain varying in length from 10 to 16 carbons are approximately identical (61), and ceramides displayed the same limiting cross-sectional area upon collapse in surface pressure studies (65). Thus, shortening of the *N*-acyl chain may have less dramatic effects on the conformation of the ceramide molecule than shortening of the sphingoid base. This could partly explain why the membrane behavior of ceramides in certain circumstances appears less sensitive to length variations in the *N*-acyl chain than in the sphingoid base. However, the use of different lipid species and molar compositions could also explain some of the discrepancies between the effects of the *N*-acyl chain and the sphingoid base observed in the studies

about chain-length-specific effects of ceramides on membrane properties.

CONCLUSIONS

The results of this study demonstrate the dependence of the membrane behavior of ceramides on the length of their sphingoid base. Shortening the length of the naturally dominant C18 sphingosine markedly affected the bilayer properties of ceramides in terms of interactions with PSM and the formation of ceramide-rich ordered- or gel-phase domains. The observed differences in the membrane behavior of the ceramides most probably originated from the chain asymmetry that caused weakening of the van der Waals interactions between the hydrocarbon chains. However, the observed effects could at least partly originate from conformational changes that weakened the hydrogen-bonding capability and lateral packing properties of the ceramides at the interfacial level. In certain circumstances, the bilayer properties of ceramides seem more sensitive to small alterations in the length of the sphingoid base than in the *N*-acyl chain, indicating possible differences in the packing properties and chain-chain interactions of these hydrocarbon chains with the acyl chains of other lipids in the center of the membrane. Altogether, the results show that the properties of the sphingoid base can lead to modified membrane properties for ceramides. In agreement with a previous suggestion by Fyrst and co-workers (41), we think that in a biological context, length variation in the sphingoid base may significantly affect the biophysical properties and biological functions of sphingolipids.

SUPPORTING MATERIAL

Two figures, one table, Materials and Methods, and supplemental references are available at [http://www.biophysj.org/biophysj/supplemental/S0006-3495\(12\)01033-8](http://www.biophysj.org/biophysj/supplemental/S0006-3495(12)01033-8)

We thank Dr. Dmitry Kuklev for valuable suggestions regarding the synthesis of tPA, Dr. Thomas Nyholm for comments on the manuscript, and Anders Kullberg for experimental assistance during the review process.

This work was supported by the Sigrid Juselius Foundation, Åbo Akademi University, National Doctoral Programme in Informational and Structural Biology, Medicinska Understödsföreningen Liv och Hälsa, Oskar Öflund Foundation, and Magnus Ehrnrooth Foundation.

REFERENCES

- Perry, D. K., and Y. A. Hannun. 1998. The role of ceramide in cell signaling. *Biochim. Biophys. Acta.* 1436:233–243.
- Hannun, Y. A., and L. M. Obeid. 2002. The ceramide-centric universe of lipid-mediated cell regulation: stress encounters of the lipid kind. *J. Biol. Chem.* 277:25847–25850.
- Taha, T. A., T. D. Mullen, and L. M. Obeid. 2006. A house divided: ceramide, sphingosine, and sphingosine-1-phosphate in programmed cell death. *Biochim. Biophys. Acta.* 1758:2027–2036.
- Hannun, Y. A., and C. Luberto. 2000. Ceramide in the eukaryotic stress response. *Trends Cell Biol.* 10:73–80.
- Cremesti, A. E., F. M. Goni, and R. Kolesnick. 2002. Role of sphingomyelinase and ceramide in modulating rafts: do biophysical properties determine biologic outcome? *FEBS Lett.* 531:47–53.
- van Blitterswijk, W. J., A. H. van der Luit, ..., J. Borst. 2003. Ceramide: second messenger or modulator of membrane structure and dynamics? *Biochem. J.* 369:199–211.
- Holopainen, J. M., J. Y. Lehtonen, and P. K. Kinnunen. 1997. Lipid microdomains in dimyristoylphosphatidylcholine-ceramide liposomes. *Chem. Phys. Lipids.* 88:1–13.
- Holopainen, J. M., M. Subramanian, and P. K. Kinnunen. 1998. Sphingomyelinase induces lipid microdomain formation in a fluid phosphatidylcholine/sphingomyelin membrane. *Biochemistry.* 37: 17562–17570.
- Hsueh, Y. W., R. Giles, ..., J. Thewalt. 2002. The effect of ceramide on phosphatidylcholine membranes: a deuterium NMR study. *Biophys. J.* 82:3089–3095.
- Massey, J. B. 2001. Interaction of ceramides with phosphatidylcholine, sphingomyelin and sphingomyelin/cholesterol bilayers. *Biochim. Biophys. Acta.* 1510:167–184.
- Silva, L., R. F. de Almeida, ..., M. Prieto. 2006. Ceramide-platform formation and -induced biophysical changes in a fluid phospholipid membrane. *Mol. Membr. Biol.* 23:137–148.
- Chiantia, S., N. Kahya, and P. Schwille. 2007. Raft domain reorganization driven by short- and long-chain ceramide: a combined AFM and FCS study. *Langmuir.* 23:7659–7665.
- Wang, T. Y., and J. R. Silvius. 2003. Sphingolipid partitioning into ordered domains in cholesterol-free and cholesterol-containing lipid bilayers. *Biophys. J.* 84:367–378.
- Alanko, S. M., K. K. Halling, ..., B. Ramstedt. 2005. Displacement of sterols from sterol/sphingomyelin domains in fluid bilayer membranes by competing molecules. *Biochim. Biophys. Acta.* 1715:111–121.
- Sot, J., M. Ibarguren, ..., A. Alonso. 2008. Cholesterol displacement by ceramide in sphingomyelin-containing liquid-ordered domains, and generation of gel regions in giant lipidic vesicles. *FEBS Lett.* 582:3230–3236.
- Westerlund, B., P. M. Grandell, ..., J. P. Slotte. 2010. Ceramide acyl chain length markedly influences miscibility with palmitoyl sphingomyelin in bilayer membranes. *Eur. Biophys. J.* 39:1117–1128.
- Nybond, S., Y. J. Björkqvist, ..., J. P. Slotte. 2005. Acyl chain length affects ceramide action on sterol/sphingomyelin-rich domains. *Biochim. Biophys. Acta.* 1718:61–66.
- Sot, J., F. J. Aranda, ..., A. Alonso. 2005. Different effects of long- and short-chain ceramides on the gel-fluid and lamellar-hexagonal transitions of phospholipids: a calorimetric, NMR, and x-ray diffraction study. *Biophys. J.* 88:3368–3380.
- Megha, P., Sawatzki, ..., E. London. 2007. Effect of ceramide *N*-acyl chain and polar headgroup structure on the properties of ordered lipid domains (lipid rafts). *Biochim. Biophys. Acta.* 1768:2205–2212.
- Nyholm, T. K., P. M. Grandell, ..., J. P. Slotte. 2010. Sterol affinity for bilayer membranes is affected by their ceramide content and the ceramide chain length. *Biochim. Biophys. Acta.* 1798:1008–1013.
- Holopainen, J. M., H. L. Brockman, ..., P. K. Kinnunen. 2001. Interfacial interactions of ceramide with dimyristoylphosphatidylcholine: impact of the *N*-acyl chain. *Biophys. J.* 80:765–775.
- Maula, T., B. Urzelai, and J. Peter Slotte. 2011. The effects of *N*-acyl chain methylations on ceramide molecular properties in bilayer membranes. *Eur. Biophys. J.* 40:857–863.
- Sot, J., F. M. Goñi, and A. Alonso. 2005. Molecular associations and surface-active properties of short- and long-*N*-acyl chain ceramides. *Biochim. Biophys. Acta.* 1711:12–19.
- Pinto, S. N., L. C. Silva, ..., M. Prieto. 2011. Effect of ceramide structure on membrane biophysical properties: the role of acyl chain length and unsaturation. *Biochim. Biophys. Acta.* 1808:2753–2760.

25. Maula, T., M. Kurita, ..., J. P. Slotte. 2011. Effects of sphingosine 2N- and 3O-methylation on palmitoyl ceramide properties in bilayer membranes. *Biophys. J.* 101:2948–2956.
26. Brockman, H. L., M. M. Momsen, ..., R. Bittman. 2004. The 4,5-double bond of ceramide regulates its dipole potential, elastic properties, and packing behavior. *Biophys. J.* 87:1722–1731.
27. Pruetz, S. T., A. Bushnev, ..., A. H. Merrill, Jr. 2008. Biodiversity of sphingoid bases (“sphingosines”) and related amino alcohols. *J. Lipid Res.* 49:1621–1639.
28. Merrill, Jr., A. H. 2002. De novo sphingolipid biosynthesis: a necessary, but dangerous, pathway. *J. Biol. Chem.* 277:25843–25846.
29. Williams, R. D., E. Wang, and A. H. Merrill, Jr. 1984. Enzymology of long-chain base synthesis by liver: characterization of serine palmitoyltransferase in rat liver microsomes. *Arch. Biochem. Biophys.* 228:282–291.
30. Merrill, Jr., A. H., D. W. Nixon, and R. D. Williams. 1985. Activities of serine palmitoyltransferase (3-ketosphinganine synthase) in microsomes from different rat tissues. *J. Lipid Res.* 26:617–622.
31. Merrill, Jr., A. H., E. Wang, and R. E. Mullins. 1988. Kinetics of long-chain (sphingoid) base biosynthesis in intact LM cells: effects of varying the extracellular concentrations of serine and fatty acid precursors of this pathway. *Biochemistry.* 27:340–345.
32. Merrill, Jr., A. H., and R. D. Williams. 1984. Utilization of different fatty acyl-CoA thioesters by serine palmitoyltransferase from rat brain. *J. Lipid Res.* 25:185–188.
33. Sonnino, S., and V. Chigorno. 2000. Ganglioside molecular species containing C18- and C20-sphingosine in mammalian nervous tissues and neuronal cell cultures. *Biochim. Biophys. Acta.* 1469:63–77.
34. Keränen, A. 1976. Fatty acids and long-chain bases of gangliosides of human gastrointestinal mucosa. *Chem. Phys. Lipids.* 17:14–21.
35. Hara, A., and T. Taketomi. 1975. Long chain base and fatty acid compositions of equine kidney sphingolipids. *J. Biochem.* 78:527–536.
36. Karlsson, A. A., P. Michélsen, and G. Odham. 1998. Molecular species of sphingomyelin: determination by high-performance liquid chromatography/mass spectrometry with electrospray and high-performance liquid chromatography/tandem mass spectrometry with atmospheric pressure chemical ionization. *J. Mass Spectrom.* 33:1192–1198.
37. Byrdwell, W. C., and R. H. Perry. 2007. Liquid chromatography with dual parallel mass spectrometry and 31P nuclear magnetic resonance spectroscopy for analysis of sphingomyelin and dihydrosphingomyelin. II. Bovine milk sphingolipids. *J. Chromatogr. A.* 1146:164–185.
38. Ramstedt, B., P. Leppimäki, ..., J. P. Slotte. 1999. Analysis of natural and synthetic sphingomyelins using high-performance thin-layer chromatography. *Eur. J. Biochem.* 266:997–1002.
39. Yunoki, K., H. Ishikawa, ..., M. Ohnishi. 2008. Chemical properties of epidermal lipids, especially sphingolipids, of the Antarctic minke whale. *Lipids.* 43:151–159.
40. Wiegandt, H. 1992. Insect glycolipids. *Biochim. Biophys. Acta.* 1123:117–126.
41. Fyrst, H., D. R. Herr, ..., J. D. Saba. 2004. Characterization of free endogenous C14 and C16 sphingoid bases from *Drosophila melanogaster*. *J. Lipid Res.* 45:54–62.
42. Farwanah, H., B. Pierstorff, ..., K. Sandhoff. 2007. Separation and mass spectrometric characterization of covalently bound skin ceramides using LC/APCI-MS and Nano-ESI-MS/MS. *J. Chromatogr. B Analyt. Technol. Biomed. Life Sci.* 852:562–570.
43. Pons, A., P. Timmerman, ..., J. P. Zanetta. 2002. Gas-chromatography/mass-spectrometry analysis of human skin constituents as heptafluorobutyrate derivatives with special reference to long-chain bases. *J. Lipid Res.* 43:794–804.
44. Maula, T., B. Westerlund, and J. P. Slotte. 2009. Differential ability of cholesterol-enriched and gel phase domains to resist benzyl alcohol-induced fluidization in multilamellar lipid vesicles. *Biochim. Biophys. Acta.* 1788:2454–2461.
45. Cohen, R., Y. Barenholz, ..., A. Dagan. 1984. Preparation and characterization of well defined D-erythro sphingomyelins. *Chem. Phys. Lipids.* 35:371–384.
46. Björkqvist, Y. J., T. K. Nyholm, ..., B. Ramstedt. 2005. Domain formation and stability in complex lipid bilayers as reported by cholesterol. *Biophys. J.* 88:4054–4063.
47. Nyström, J. H., M. Lönnfors, and T. K. Nyholm. 2010. Transmembrane peptides influence the affinity of sterols for phospholipid bilayers. *Biophys. J.* 99:526–533.
48. Castro, B. M., R. F. de Almeida, ..., M. Prieto. 2007. Formation of ceramide/sphingomyelin gel domains in the presence of an unsaturated phospholipid: a quantitative multiprobe approach. *Biophys. J.* 93:1639–1650.
49. Silva, L. C., R. F. de Almeida, ..., M. Prieto. 2007. Ceramide-domain formation and collapse in lipid rafts: membrane reorganization by an apoptotic lipid. *Biophys. J.* 92:502–516.
50. Castro, B. M., L. C. Silva, ..., M. Prieto. 2009. Cholesterol-rich fluid membranes solubilize ceramide domains: implications for the structure and dynamics of mammalian intracellular and plasma membranes. *J. Biol. Chem.* 284:22978–22987.
51. Busto, J. V., M. L. Fanani, ..., A. Alonso. 2009. Coexistence of immiscible mixtures of palmitoylsphingomyelin and palmitoylceramide in monolayers and bilayers. *Biophys. J.* 97:2717–2726.
52. Sot, J., L. A. Bagatolli, ..., A. Alonso. 2006. Detergent-resistant, ceramide-enriched domains in sphingomyelin/ceramide bilayers. *Biophys. J.* 90:903–914.
53. Halling, K. K., B. Ramstedt, ..., T. K. Nyholm. 2008. Cholesterol interactions with fluid-phase phospholipids: effect on the lateral organization of the bilayer. *Biophys. J.* 95:3861–3871.
54. de Almeida, R. F., A. Fedorov, and M. Prieto. 2003. Sphingomyelin/phosphatidylcholine/cholesterol phase diagram: boundaries and composition of lipid rafts. *Biophys. J.* 85:2406–2416.
55. Megha, and E. London. 2004. Ceramide selectively displaces cholesterol from ordered lipid domains (rafts): implications for lipid raft structure and function. *J. Biol. Chem.* 279:9997–10004.
56. Yu, C., M. Alterman, and R. T. Dobrowsky. 2005. Ceramide displaces cholesterol from lipid rafts and decreases the association of the cholesterol binding protein caveolin-1. *J. Lipid Res.* 46:1678–1691.
57. Tsamaloukas, A., H. Szadkowska, and H. Heerklotz. 2006. Thermodynamic comparison of the interactions of cholesterol with unsaturated phospholipid and sphingomyelins. *Biophys. J.* 90:4479–4487.
58. Cevc, G. 1991. How membrane chain-melting phase-transition temperature is affected by the lipid chain asymmetry and degree of unsaturation: an effective chain-length model. *Biochemistry.* 30:7186–7193.
59. Pascher, I. 1976. Molecular arrangements in sphingolipids. Conformation and hydrogen bonding of ceramide and their implication on membrane stability and permeability. *Biochim. Biophys. Acta.* 455:433–451.
60. Reference deleted in proof.
61. Karttunen, M., M. P. Haataja, ..., J. M. Holopainen. 2009. Lipid domain morphologies in phosphatidylcholine-ceramide monolayers. *Langmuir.* 25:4595–4600.
62. Kodama, M., and Y. Kawasaki. 2010. Structural role of mismatched C-C bonds in a series of d-erythro-sphingomyelins as studied by DSC and electron microscopy. *Chem. Phys. Lipids.* 163:514–523.
63. Jaikishan, S., and J. P. Slotte. 2011. Effect of hydrophobic mismatch and interdigitation on sterol/sphingomyelin interaction in ternary bilayer membranes. *Biochim. Biophys. Acta.* 1808:1940–1945.
64. Carrer, D. C., S. Schreier, ..., B. Maggio. 2006. Effects of a short-chain ceramide on bilayer domain formation, thickness, and chain mobility: DMPC and asymmetric ceramide mixtures. *Biophys. J.* 90:2394–2403.
65. Dupuy, F., and B. Maggio. 2012. The hydrophobic mismatch determines the miscibility of ceramides in lipid monolayers. *Chem. Phys. Lipids.* 165:615–629.
66. Löfgren, H., and I. Pascher. 1977. Molecular arrangements of sphingolipids. The monolayer behaviour of ceramides. *Chem. Phys. Lipids.* 20:273–284.